Internal Report
DESY D3-62
December 1987

# DATA ON MUON DOSES BEHIND THICK SHIELDING AT ELECTRON ACCELERATORS

by

E. Bräuer, K. Tesch

Internal Report
DESY-D3-62
December 1987

# Data on muon doses behind thick shielding at electron accelerators

E. Bräuer and K. Tesch

## Abstract

The muon dose behind a thick shield and at zero degree with respect to an incoming electron beam was calculated using a theoretical expression developed by W.R. Nelson. Soil, ordinary concrete, heavy concrete, aluminium, iron and lead were considered as shielding materials, and the electron beam energy was varied between 1 and 50 GeV. In addition, some informations are given regarding the angular spread of the produced muon beam, the effect of ranging the distance between target and muon shield and the use of a shield composed of two different materials. Results are compared with a simple approximate formula given by W.P. Swanson.

Muons are the most penetrating particles to be considered in shielding calculations at high energy accelerators. At muon energies of less than fifty GeV ionisation losses and scattering effects are the only attenuating processes. Around electron accelerators, muons arise from pair production and their production cross sections are known; in fact several different approximations have been made by various authors. Since the attenuating processes are also understood theoretically, the flux of muons and hence the dose are calculable in principle behind any given shield.

The first comprehensive dose calculations were performed by Nelson [1] with the geometry as shown in figure 1. It was herein assumed that the electromagnetic cascade in the target was completely developed. The track length formula by Clement and Kessler was used. The angular distribution of photons in the cascade was neglected. For the doubly differential production cross-section a simple expression by Tsai was substituted which is only valid for small angles, moreover no form factor was taken into account. Fermi-Eyges theory provided a basis for treating multiple scattering.

Nelson compared his calculations with measurements, taking an 18 GeV electron beam, 4.3 m of iron and angles no greater than 60 mrad. Within this angular range an agreement of better than a factor 2 on an absolute basis was reached; the theoretical dose distribution was narrower so that at zero angle the calculated dose values exceeded that measured and at larger angles they were smaller.

In two succeeding papers [2,3] Nelson and collaborators presented an improved theory. The most significant enhancement was to take the production cross-section of Kim and Tsai. These authors considered coherent production from the nucleus and the elastic part of incoherent production from the protons, the respective form factors were taken into account. When compared with another shielding experiment done at 18 GeV, behind 5 to 7 m of iron, the improved calculation gave smaller dose values than in the first approach and better agreement with the experiment at small angles. There was good agreement, in fact of less than 20% deviation from the experimental result at zero degree and up to that angle where the dose is a factor of ten less than the zero degree value. For larger angles the theoretical results are again too low when compared with measurements.

In order to have muon dose data at hand and since no other theoretical or experimental investigations are known, we found it useful to evaluate Nelson's

theory in the energy region of interest, i.e. for electron energies between 1 and 50 GeV and for shielding materials most frequently used (lead, iron, aluminium, heavy concrete, ordinary concrete and soil).

Given good agreement at 18 GeV the calculations may also be sufficient for shielding estimates at other energies. Unfortunately the theory in ref. 2 is very tedious to evaluate. Therefore we used the much simpler expression in ref. 1 and multiplied the results by a factor 0.6 to have agreement with the experiment at 18 GeV and in the angular range mentioned above. The same factor was used at all other energies, though this procedure is not justified by any theoretical consideration. Nevertheless we believe that the results are good enough for health physics purposes.

Nelson's theory [1] is essentially a fourfold integral to be evaluated numerically. We used the stopping power values and muon ranges supplied in refs. 4-7. Mean values were taken in energy regions where the data sets of the various authors are overlapping which is justified by the differences in value being small, no more than 10% even at 50 GeV. The final values are listed in table 1 and 2, and the mean composition of concretes and soil are given in table 3.

In what follows we present the results of our calculations.

Figures 2 to 13 show muon doses at zero degree in cGray (rad) per incoming electron, plotted against material thickness (in g $cm^{-2}$) for six different shielding materials and for electron energies between 1 and 50 GeV. The electron beam is assumed to impinge directly on the shielding material, i.e. r = d in fig. 1. Each arrow at the bottom of a figure indicates the maximum muon range.

The produced muon beam is sharply directed into the forward direction. To indicate its lateral distribution we additionally calculated the angle $\Theta_{1/10}$ at which the dose is 10% of the dose at zero degree, for a shielding thickness which is 50% of the maximum muon range at each electron energy. Figure 14 shows these values plotted against electron energy and demonstrates clearly that with increasing energy the angular distribution of dose becomes narrower, due to decreasing production angles and smaller scattering effects. $\Theta_{1/10}$ is only weakly dependent on the shielding thickness. If the thickness varies

between 10% and 90% of the muon range, $\Theta_{1/10}$ differs by not more than 25% from the value given in fig. 14.

In fig. 2 to 13 we assumed that the electron hits directly the shielding wall. In practice the target in which the electromagnetic cascade develops (e.g. an accelerator component or a lead absorber) is often separated from the muon shield, i.e. r > d in fig. 1. For this case a simple $1/r^2$-dependence of the muon dose at zero degree is expected if the spread of the muon beam in the shield due to multiple scattering can be neglected compared with the angular distribution of muons produced in the target; if the opposite is true the muon dose should be independent of r. We studied this r-dependence for iron shields of three different thicknesses and for electron energies between 3 GeV and 30 GeV, the results are shown in fig. 15 (R = maximum range of muons), they agree with our qualitative expectations.

In practice it is often convenient to make the electron beam absorber thick enough to absorb most of its energy in order to keep the activation of material within a finite volume. In this case the muon shield is composed of two layers, e.g. lead or iron and behind this a shield of concrete or sand. It is expected that such a shield is less effective than a shield of the same thickness (expressed in g $cm^{-2}$) and composed of sand or concrete only because of the smaller stopping power per g $cm^{-2}$ of the heavier material and the smaller geometrical extention. To get an impression of this effect we calculated the dose at zero degree behind a shield composed of 40 cm lead and sand and compared it with a pure sand shield in figs. 16 and 17. In table 4 muon doses are given behind a concrete shield and behind a combination of concrete and heavier materials.

Finally we compared our results with an approximate formula given by Swanson [8]

$$H(d) = H_o \cdot [25(25+d/X_o)^{-1}] \cdot [(R-d) \cdot R^{-1}]$$

where $H(d)$: dose rate behind shield with thickness d at $0^o$

$H_o$ : dose rate without shield

d : thickness

$X_o$ : radiation length

R : muon range at energy $E_o$.

$H_o$ is presented in fig. 18 which shows the unshielded dose-equivalent rate $H_o$ normalized to 1 m per unit electron beam power as a function of the electron energy $E_o$.

In order to compare his approximation with our results, the formula was rewritten to give the dose in cGray per electron:

$$H(d) = [(4.44 \cdot 10^{-13} H_o E_o \cdot \rho^2) \cdot d^{-2}] \cdot [25(25+d/X_o)^{-1}] \cdot [(R-d) \cdot R^{-1}]$$

where $H(d)$ and $H_o$ are in cGray, $E_o$ in GeV, density $\rho$ in $g \cdot cm^{-3}$ and $d$ in $g \cdot cm^{-2}$.

At 5 GeV and for all shielding materials studied, the agreement between Swanson's formula and the results from Nelson's theory is better than a factor of two up to a thickness corresponding to half of the maximum muon range; at 30 GeV the agreement is better than a factor of 1.5. For a thickness higher than half of the respective maximum muon range, Swanson's formula gives a strong overestimation of the muon dose.

References

[1] W.R. Nelson
The shielding of muons around high energy electron accelerators: theory and measurement
Nucl. Instr. Meth. 66, 293 (1968)

[2] W.R. Nelson and K.R. Kase
Muon shielding around high energy electron accelerators. Part I, Theory
Nucl. Instr. Meth. 120, 401 (1974)

[3] W.R. Nelson, K.R. Kase and G.K. Svensson
Muon shielding around high energy electron accelerators. Part II, Experimental Investigation
Nucl. Instr. Meth. 120, 413 (1974)

[4] W.H. Barkas and M.J. Berger
Tables of Energy Losses and Ranges of Heavy Charged Particles
National Bureau of Standards, Washington D.C., NASA SP-3013 (1964)

[5] D. Theriot
Muon dE/dx and Range Tables
Fermi-National Accelerator Laboratory
Internal Report TM-260 (1970)

[6] C. Richard-Serre
Evaluation de la Perte d'Energie Unitaire et du Parcours pour des Muons de 2 à 600 GeV dans un Absorbant Quelconque
CERN 71-18 (1971)

[7] G.R. Stevenson
Calculations of dE/dx and muon ranges in concrete and earth
CERN Internal Report TIS-RP/iR/84-07 (1984)

[8] W.P. Swanson
Radiological Safety Aspects of the Operation of Electron Linear Accelerators
IAEA Technical Reports Series No. 188 (1979)

| T (GeV) | Al | Fe | Pb | Soil | OCONC | HCONC |
|---|---|---|---|---|---|---|
| 0.002 | 21.657 | 18.814 | 10.583 | 23.74 | 24.39 | 21.47 |
| 0.004 | 12.567 | 11.073 | 7.181 | 13.70 | 14.07 | 12.50 |
| 0.006 | 9.160 | 8.126 | 5.431 | 9.954 | 10.225 | 10.44 |
| 0.008 | 7.348 | 6.545 | 4.455 | 7.967 | 8.148 | 7.316 |
| 0.01 | 6.216 | 5.552 | 3.826 | 6.727 | 6.910 | 6.187 |
| 0.014 | 4.827 | 4.368 | 3.057 | 5.270 | 5.414 | 4.943 |
| 0.018 | 4.097 | 3.683 | 2.603 | 4.414 | 4.535 | 4.076 |
| 0.022 | 3.593 | 3.236 | 2.303 | 3.875 | 3.981 | 3.582 |
| 0.026 | 3.240 | 2.921 | 2.090 | 3.486 | 3.581 | 3.170 |
| 0.03 | 2.977 | 2.688 | 1.931 | 3.206 | 3.294 | 2.969 |
| 0.034 | 2.776 | 2.509 | 1.809 | 2.985 | 3.066 | 2.765 |
| 0.038 | 2.617 | 2.367 | 1.711 | 2.815 | 2.891 | 2.609 |
| 0.042 | 2.489 | 2.253 | 1.633 | 2.673 | 2.746 | 2.480 |
| 0.046 | 2.383 | 2.157 | 1.568 | 2.557 | 2.672 | 2.373 |
| 0.05 | 2.294 | 2.079 | 1.517 | 2.471 | 2.530 | 2.264 |
| 0.06 | 2.121 | 1.929 | 1.411 | 2.285 | 2.344 | 2.100 |
| 0.07 | 2.005 | 1.821 | 1.340 | 2.158 | 2.214 | 1.982 |
| 0.08 | 1.920 | 1.743 | 1.285 | 2.068 | 2.121 | 1.901 |
| 0.09 | 1.857 | 1.690 | 1.251 | 1.980 | 2.051 | 1.840 |
| 0.1 | 1.808 | 1.643 | 1.221 | 1.942 | 1.997 | 1.791 |
| 0.11 | 1.770 | 1.611 | 1.200 | 1.902 | 1.956 | 1.752 |
| 0.14 | 1.696 | 1.543 | 1.161 | 1.824 | 1.878 | 1.683 |
| 0.42 | 1.637 | 1.501 | 1.170 | 1.774 | 1.847 | 1.643 |
| 0.66 | 1.687 | 1.551 | 1.225 | 1.790 | 1.847 | 1.640 |
| 0.94 | 1.738 | 1.601 | 1.278 | 1.850 | 1.900 | 1.700 |
| 1.4 | 1.802 | 1.657 | 1.342 | 1.910 | 1.952 | 1.76 |
| 2.0 | 1.851 | 1.711 | 1.397 | 1.967 | 2.051 | 1.81 |
| 2.8 | 1.882 | 1.761 | 1.439 | 2.013 | 2.097 | 1.86 |
| 3.6 | 1.905 | 1.804 | 1.492 | 2.064 | 2.189 | 1.90 |
| 5.0 | 1.999 | 1.852 | 1.539 | 2.111 | 2.192 | 1.95 |
| 8.0 | 2.058 | 1.913 | 1.613 | 2.180 | 2.265 | 2.01 |
| 12 | 2.120 | 1.973 | 1.686 | 2.242 | 2.326 | 2.06 |
| 15 | 2.154 | 2.007 | 1.726 | 2.269 | 2.361 | 2.09 |
| 20 | 2.203 | 2.053 | 1.787 | 2.309 | 2.409 | 2.12 |
| 25 | 2.242 | 2.089 | 1.844 | 2.338 | 2.449 | 2.13 |
| 30 | 2.275 | 2.119 | 1.889 | 2.371 | 2.484 | 2.16 |
| 35 | 2.306 | 2.145 | 1.934 | 2.390 | 2.515 | 2.17 |
| 40 | 2.334 | 2.170 | 1.979 | 2.410 | 2.545 | 2.18 |
| 45 | 2.361 | 2.194 | 2.023 | 2.427 | 2.572 | 2.19 |
| 50 | 2.387 | 2.219 | 2.067 | 2.445 | 2.598 | 2.20 |

Table 1: Stopping power values dE/dx in $MeV \cdot cm^2 \cdot g^{-1}$.

| T (GeV) | Al | Fe | Pb |
|---|---|---|---|
| 0.03 | 6.06 | 6.75 | 9.62 |
| 0.07 | 23.26 | 25.7 | 35.7 |
| 0.1 | 39.12 | 43.2 | 59.2 |
| 0.3 | 159.8 | 175.5 | 233.3 |
| 0.5 | 282.2 | 309.0 | 405.7 |
| 1.0 | 575.9 | 629.0 | 809.2 |
| 3.6 | 1972 | 2139 | 2649 |
| 7.0 | 3679 | 3968 | 4857 |
| 10 | 5128 | 5522 | 6696 |
| 15 | 7475 | 8035 | 9621 |
| 20 | 9764 | 10474 | 12415 |
| 25 | 12010 | 12872 | 15136 |
| 30 | 14219 | 15206 | 17758 |
| 35 | 16435 | 17685 | 20625 |
| 40 | 18589 | 19996 | 22876 |
| 45 | 20720 | 22290 | 25755 |
| 50 | 22824 | 24567 | 28254 |

| T (GeV) | Soil | OCONC | HCONC |
|---|---|---|---|
| 0.03 | 5.60 | 5.45 | 6.15 |
| 0.07 | 21.64 | 21.06 | 23.57 |
| 0.1 | 36.37 | 35.40 | 39.59 |
| 0.3 | 147.5 | 144 | 161.25 |
| 0.5 | 257 | 250 | 282 |
| 1.0 | 525 | 526 | 575 |
| 3.6 | 1825 | 1773 | 1965 |
| 7.0 | 3409 | 3324 | 3650 |
| 10 | 4751 | 4624 | 5085 |
| 15 | 7027 | 6753 | 7420 |
| 20 | 9052 | 8828 | 9690 |
| 25 | 11160 | 10873 | 11950 |
| 30 | 13201 | 12866 | 14200 |
| 35 | 15460 | 15000 | 17050 |
| 40 | 17500 | 16985 | 19300 |
| 45 | 19510 | 18940 | 21750 |
| 50 | 21509 | 20885 | 23900 |

Table 2: Muon ranges R in $g \cdot cm^{-2}$.

| Elements | heavy concrete | ordinary concrete | soil |
|---|---|---|---|
| O | 0.33 | 0.51 | 0.55 |
| Si | 0.05 | 0.28 | 0.3 |
| Ca | 0.05 | 0.13 | 0.07 |
| Fe | 0.57 | 0.02 | 0.03 |
| C | - | 0.03 | - |
| H | - | - | 0.02 |
| Al | - | 0.03 | 0.03 |

Table 3: Composition of heavy concrete, ordinary concrete and soil in parts by weight.

| Shielding material | Dose (cGray/$e^-$) | |
|---|---|---|
| | 5 GeV | 30 GeV |
| 2000 g·cm$^{-2}$ OCONC | $0.86 \cdot 10^{-19}$ | $0.648 \cdot 10^{-15}$ |
| 1300 g·cm$^{-2}$ OCONC + 700 g·cm$^{-2}$ Fe | $0.445 \cdot 10^{-18}$ | $0.118 \cdot 10^{-14}$ |
| 1300 g·cm$^{-2}$ OCONC + 700 g·cm$^{-2}$ Pb | $0.945 \cdot 10^{-18}$ | $0.124 \cdot 10^{-14}$ |

Table 4: Muon doses behind a concrete shield and behind a combination of concrete and heavier materials for 5 and 30 GeV.

Figure Captions

Fig. 1 Shielding diagram showing the geometry with source point at T and the angle $\Theta$.

Fig. 2-13 Muon doses at zero degree in cGray per incoming electron, plotted against material thickness (in $g \cdot cm^{-2}$) for six different shielding materials and for electron energies between 1 an 50 GeV.

Fig. 14 $\Theta_{1/10}$-values in radian plotted against electron energy.

Fig. 15 Dependence of the muon dose on distance r for 3 fixed shielding thicknesses d (see fig.1) and for 3 electron energies $E_o$. R = maximum muon range.

Fig. 16 +17 Muon doses at zero degree behind a pure soil shield and behind a shield of soil and 40 cm lead for 5 GeV and 30 GeV.

Fig. 18 Muon production at 0° from an unshielded thick iron target, as a function of electron energy $E_o$ (adapted from W. Swanson [8]).

FIG. 1

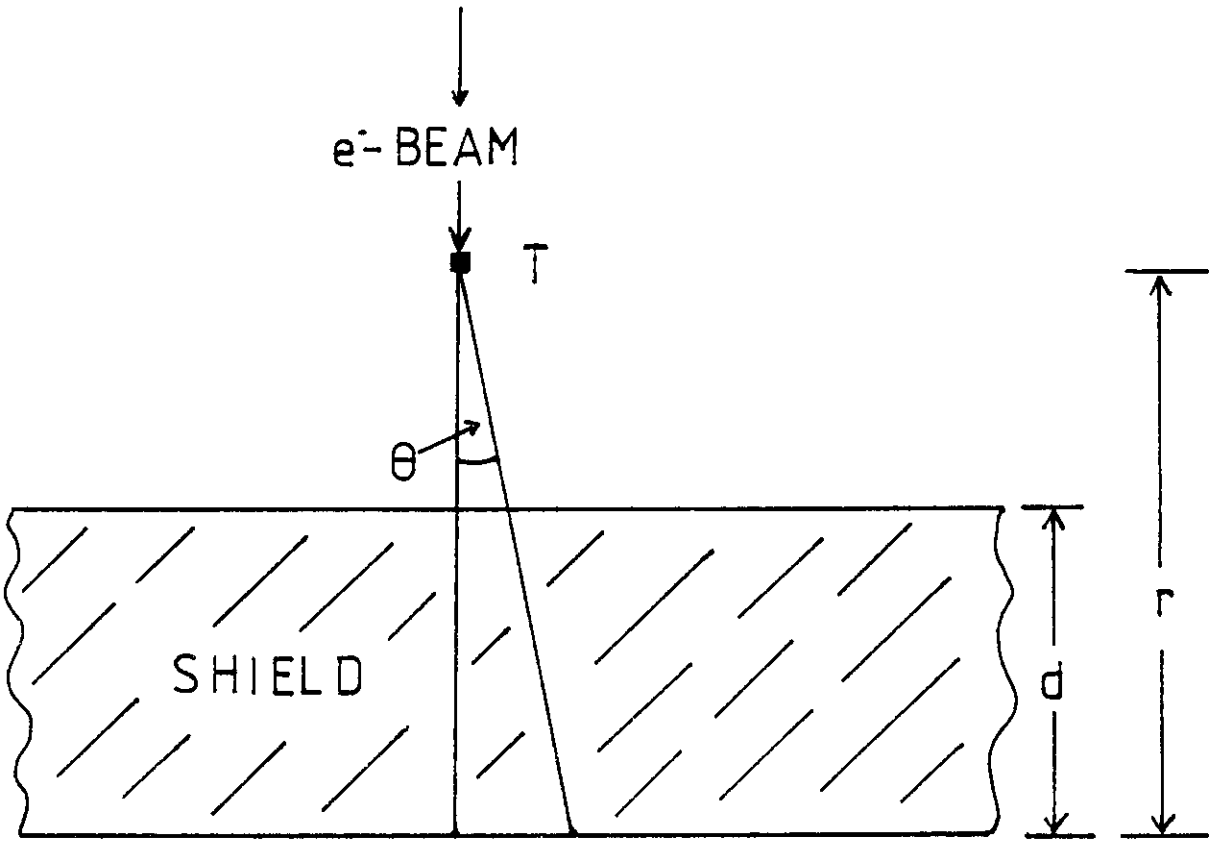

FIG. 2

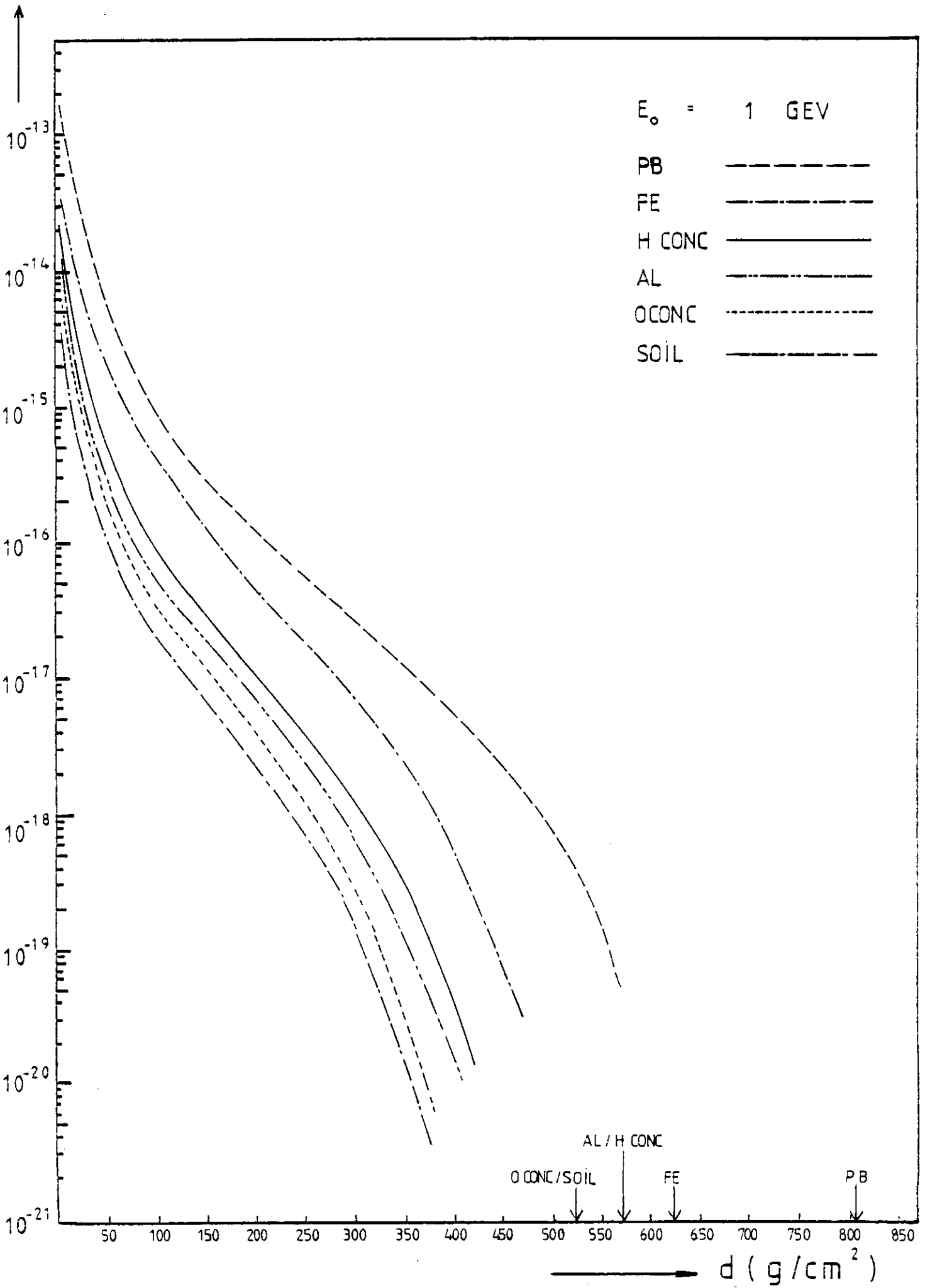
DOSE (cGray/e⁻)
E₀ = 1 GEV
PB
FE
H CONC
AL
OCONC
SOIL
10⁻¹³
10⁻¹⁴
10⁻¹⁵
10⁻¹⁶
10⁻¹⁷
10⁻¹⁸
10⁻¹⁹
10⁻²⁰
10⁻²¹
AL / H CONC
O CONC/SOIL
FE
PB
50 100 150 200 250 300 350 400 450 500 550 600 650 700 750 800 850
d ( g/cm² )

DOSE (cGray/e⁻)

FIG. 3

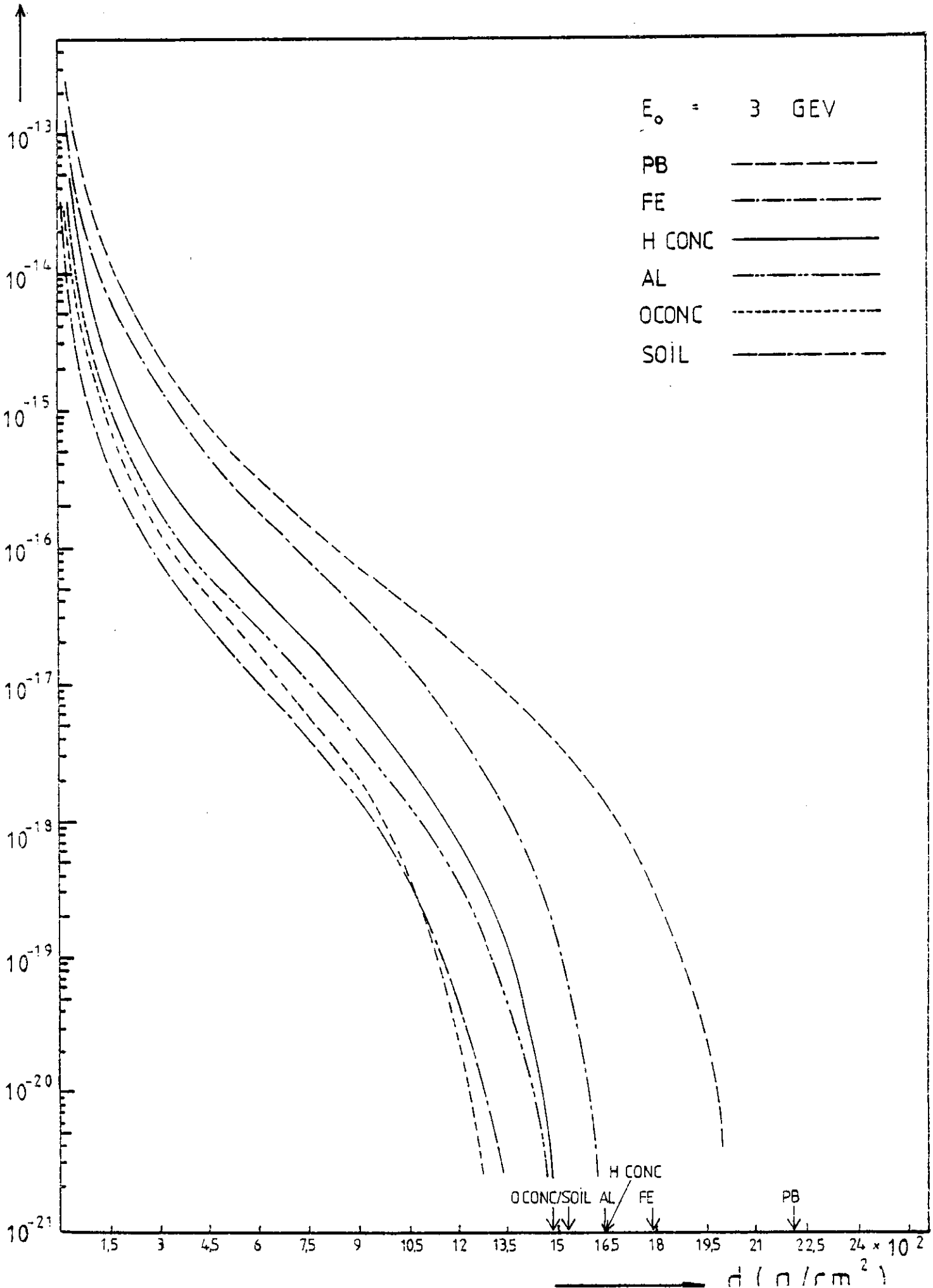

FIG. 4

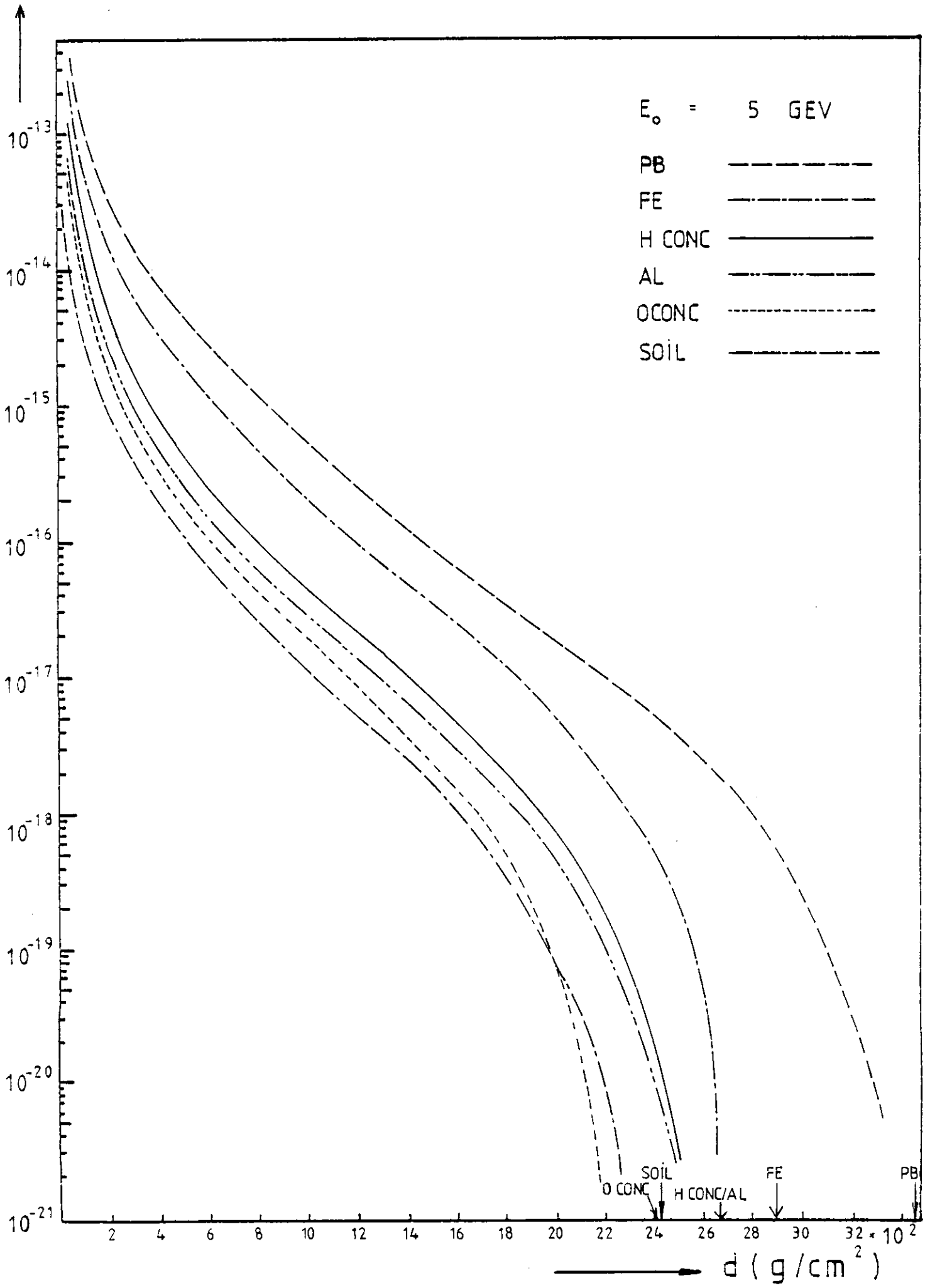
DOSE (cGray/e⁻)
E₀ = 5 GEV
PB
FE
H CONC
AL
OCONC
SOIL
10⁻¹³
10⁻¹⁴
10⁻¹⁵
10⁻¹⁶
10⁻¹⁷
10⁻¹⁸
10⁻¹⁹
10⁻²⁰
10⁻²¹
O CONC
SOIL
H CONC/AL
FE
PB
2 4 6 8 10 12 14 16 18 20 22 24 26 28 30 32 × 10²
d (g/cm²)

DOSE (cGray/e⁻)

FIG. 5

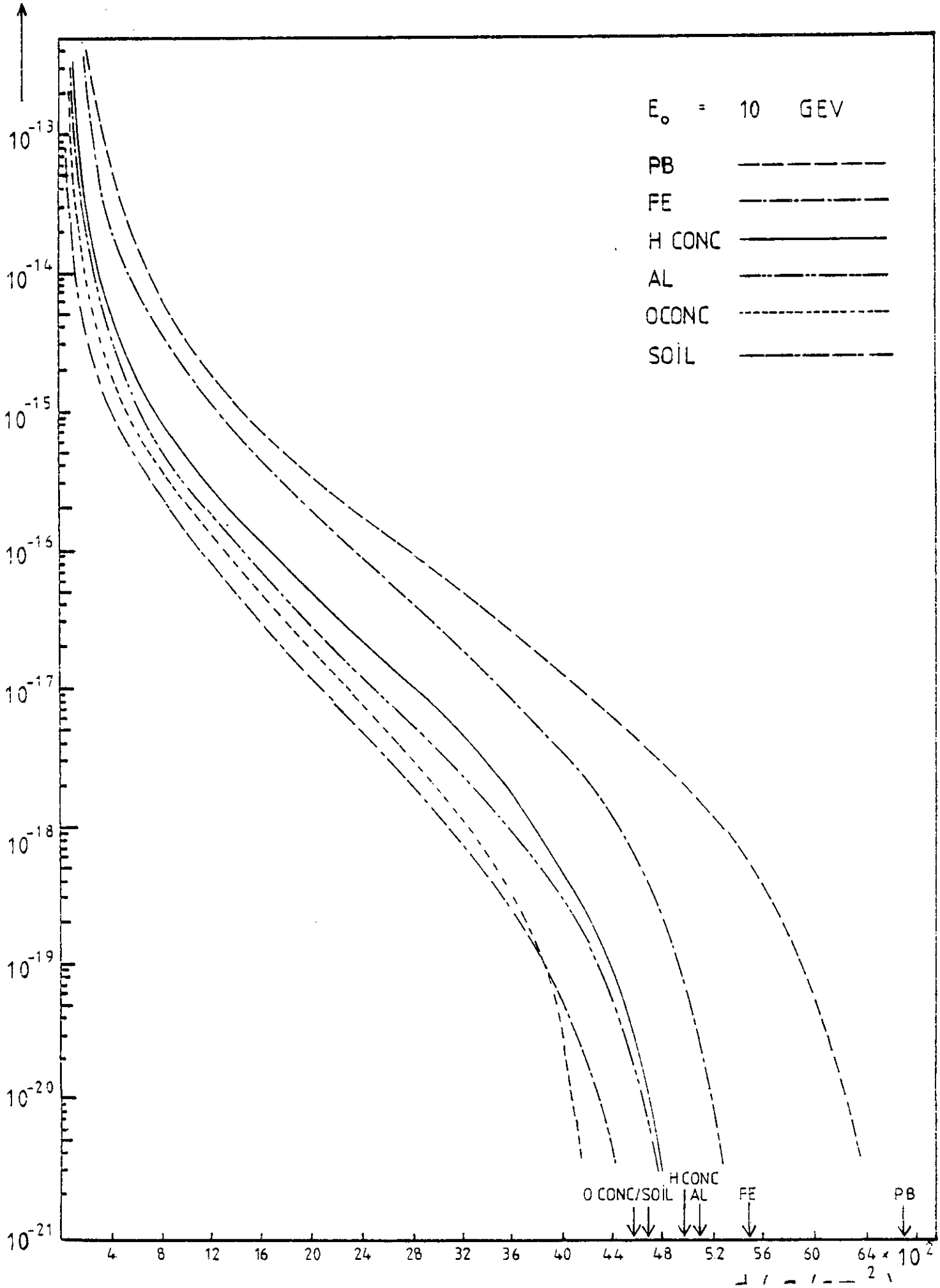

FIG. 6

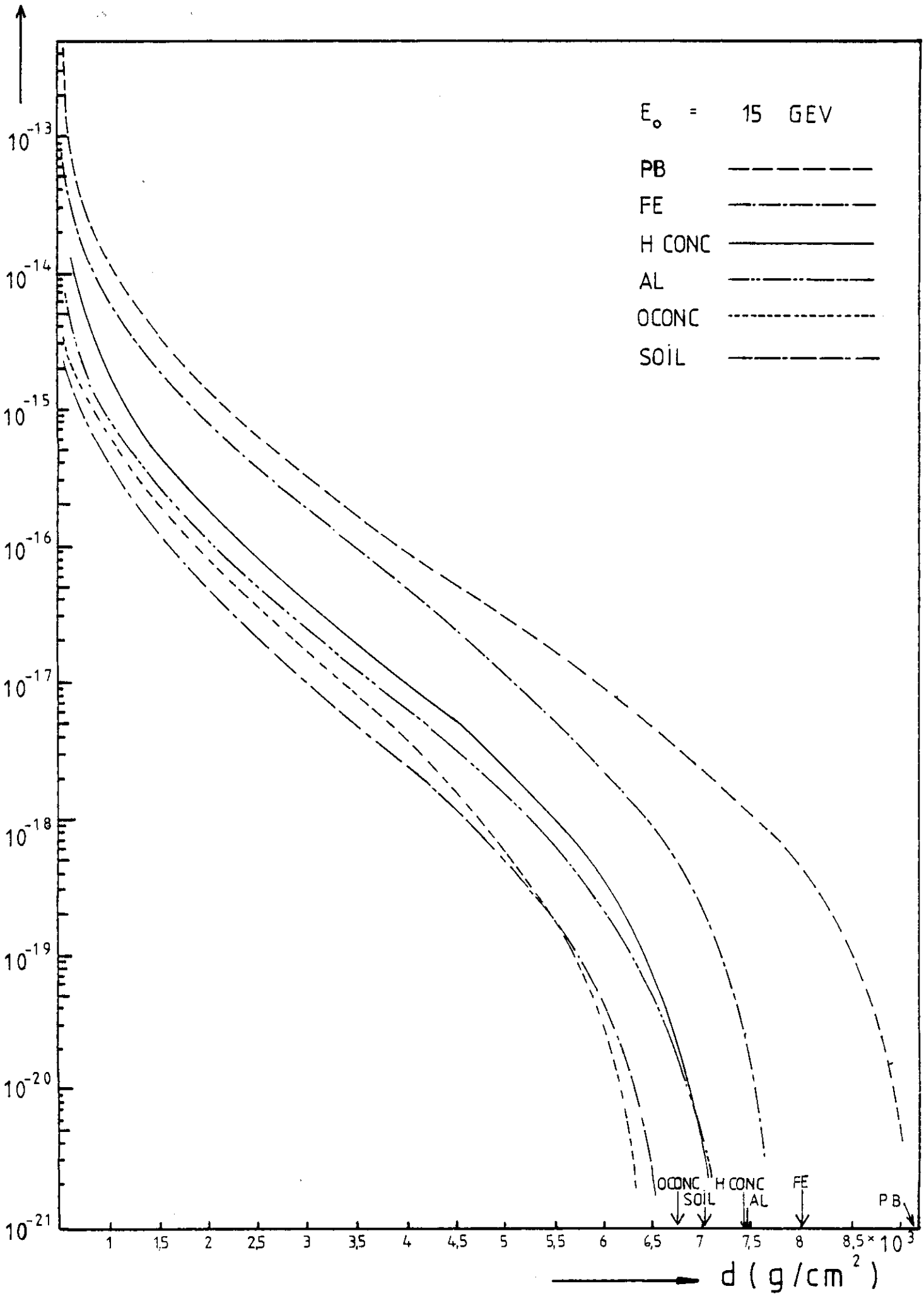
DOSE (cGray/e⁻)
E₀ = 15 GEV
PB
FE
H CONC
AL
OCONC
SOIL
10⁻¹³
10⁻¹⁴
10⁻¹⁵
10⁻¹⁶
10⁻¹⁷
10⁻¹⁸
10⁻¹⁹
10⁻²⁰
10⁻²¹
1
1,5
2
2,5
3
3,5
4
4,5
5
5,5
6
6,5
7
7,5
8
8,5 × 10³
OCONC
SOIL
H CONC
AL
FE
PB
d (g/cm²)

DOSE (cGray/e⁻)

FIG. 7

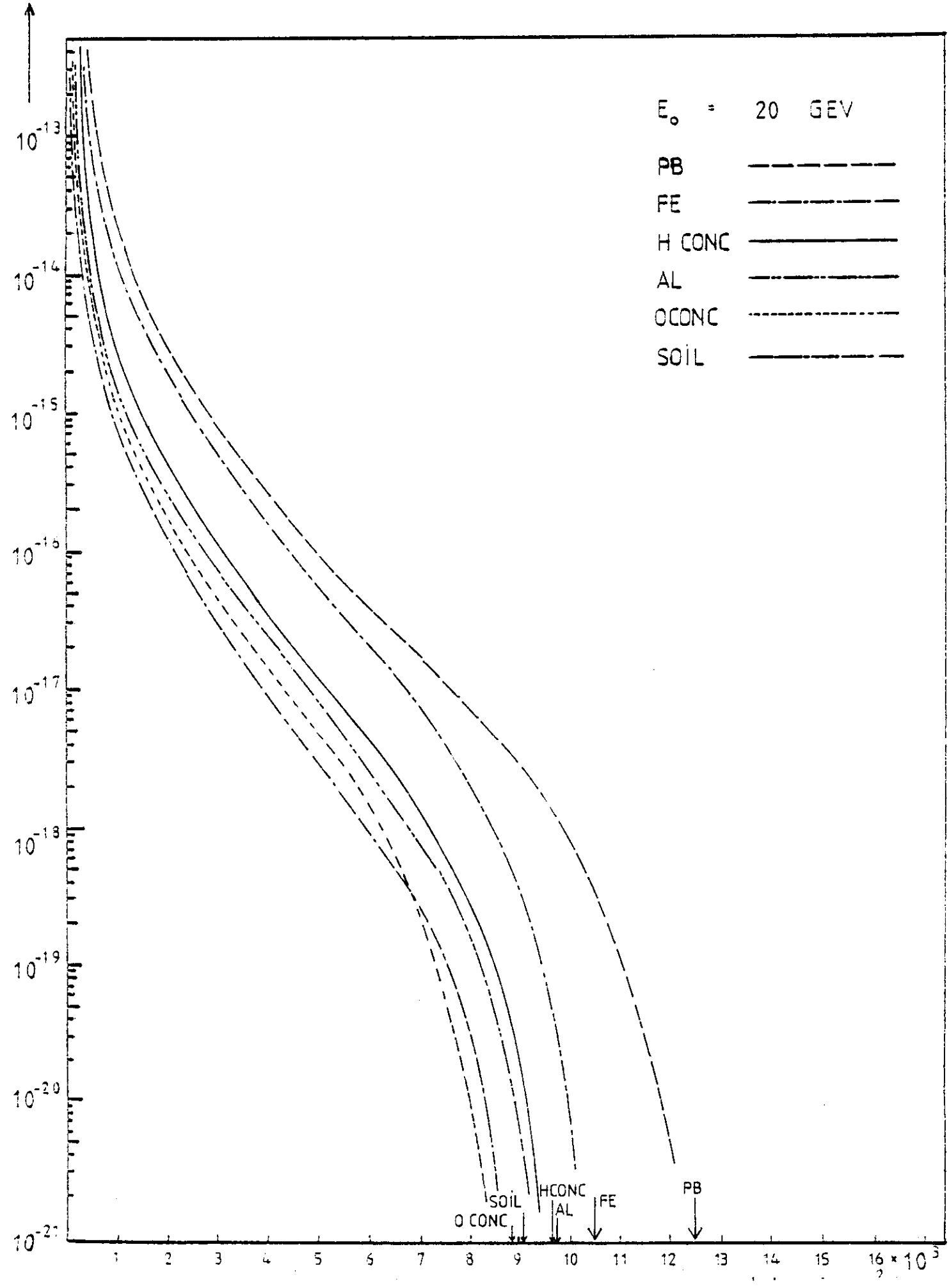

FIG. 8

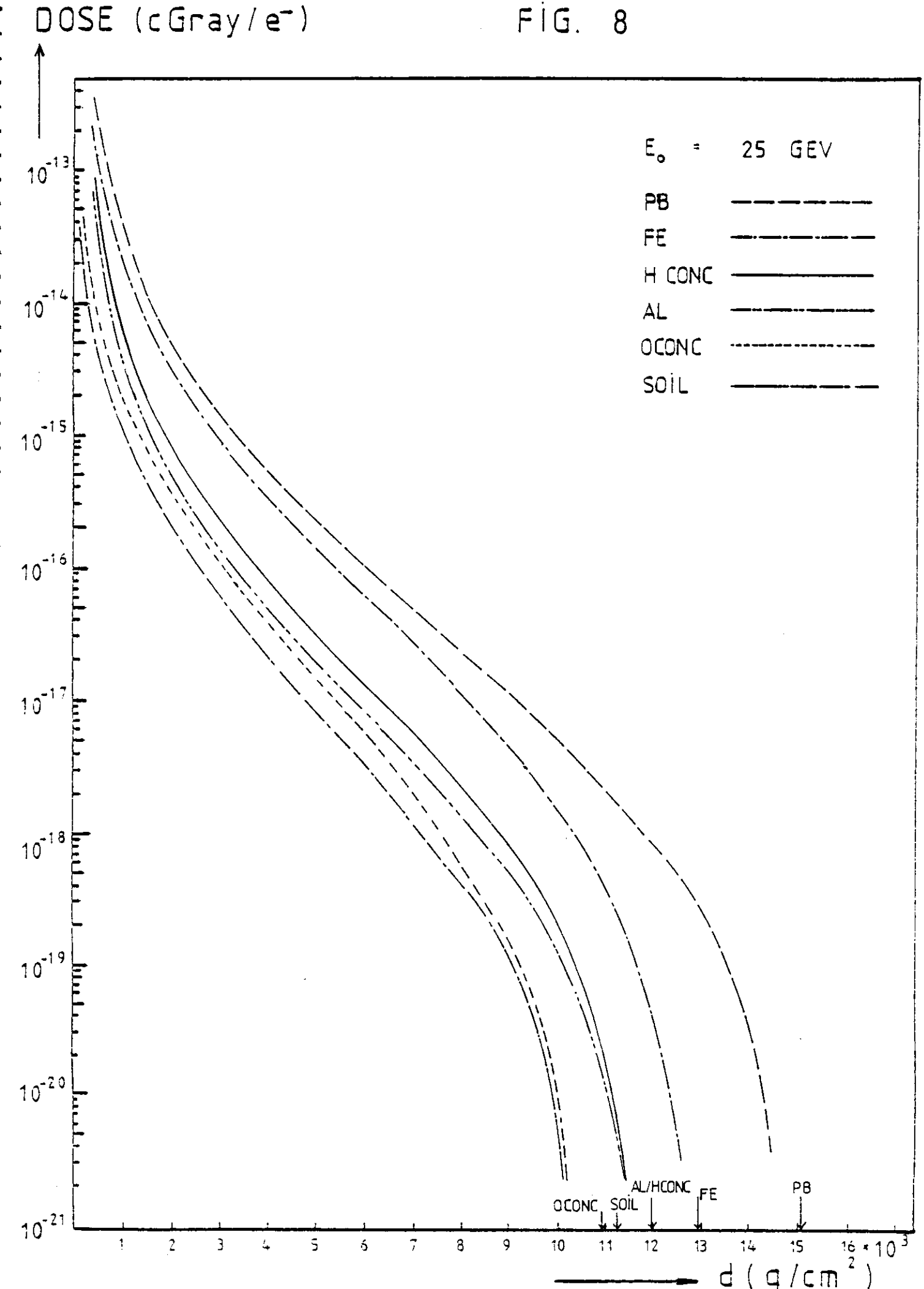
DOSE (cGray/e⁻)
$E_o$ = 25 GEV
PB
FE
H CONC
AL
OCONC
SOIL
$10^{-13}$
$10^{-14}$
$10^{-15}$
$10^{-16}$
$10^{-17}$
$10^{-18}$
$10^{-19}$
$10^{-20}$
$10^{-21}$
OCONC
SOIL
AL/HCONC
FE
PB
1 2 3 4 5 6 7 8 9 10 11 12 13 14 15 16 × $10^3$
d ( g/cm$^2$ )

DOSE (cGray/e⁻)

FIG. 9

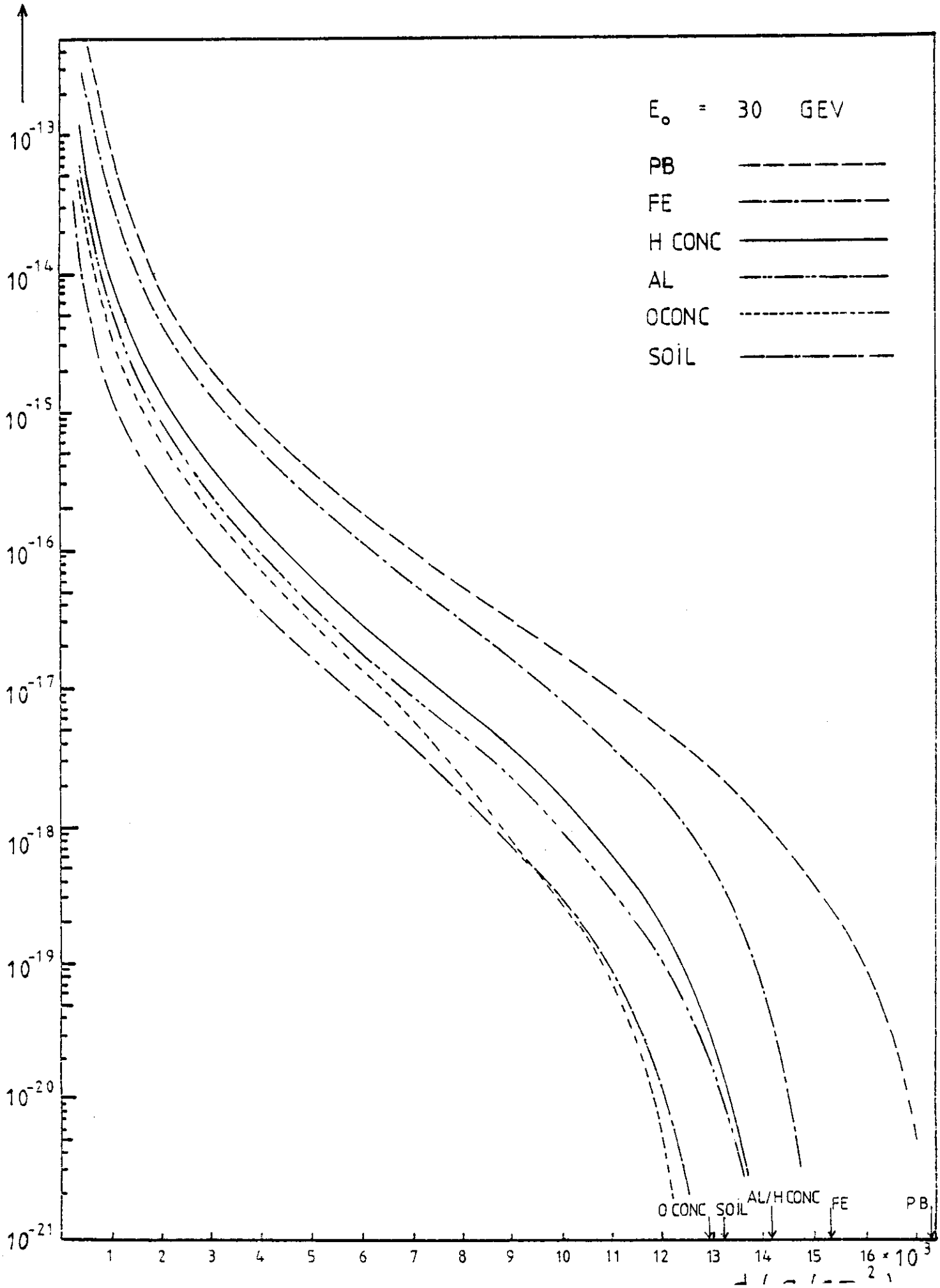

DOSE (cGray/e⁻)

FIG. 10

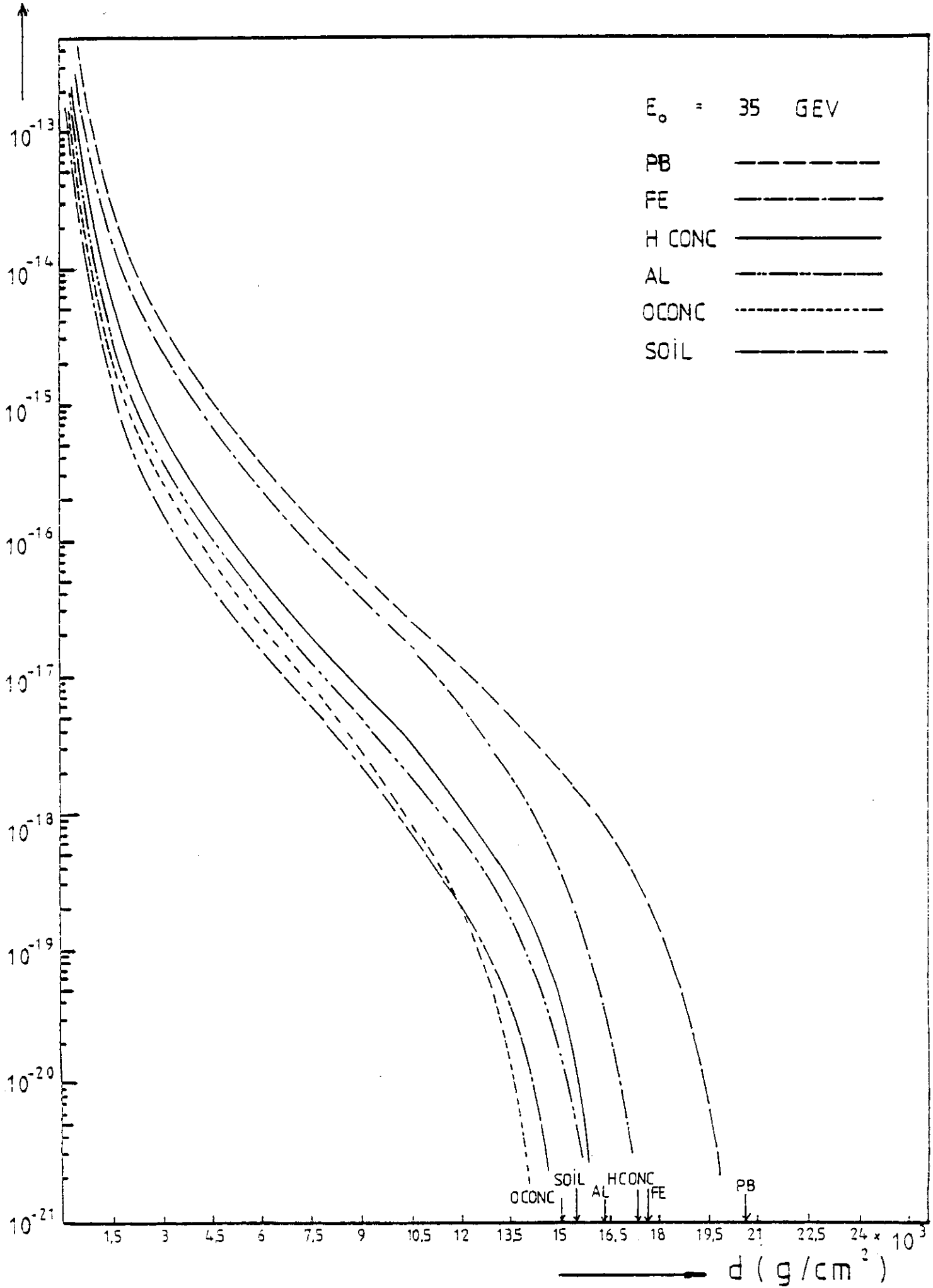

FIG. 11

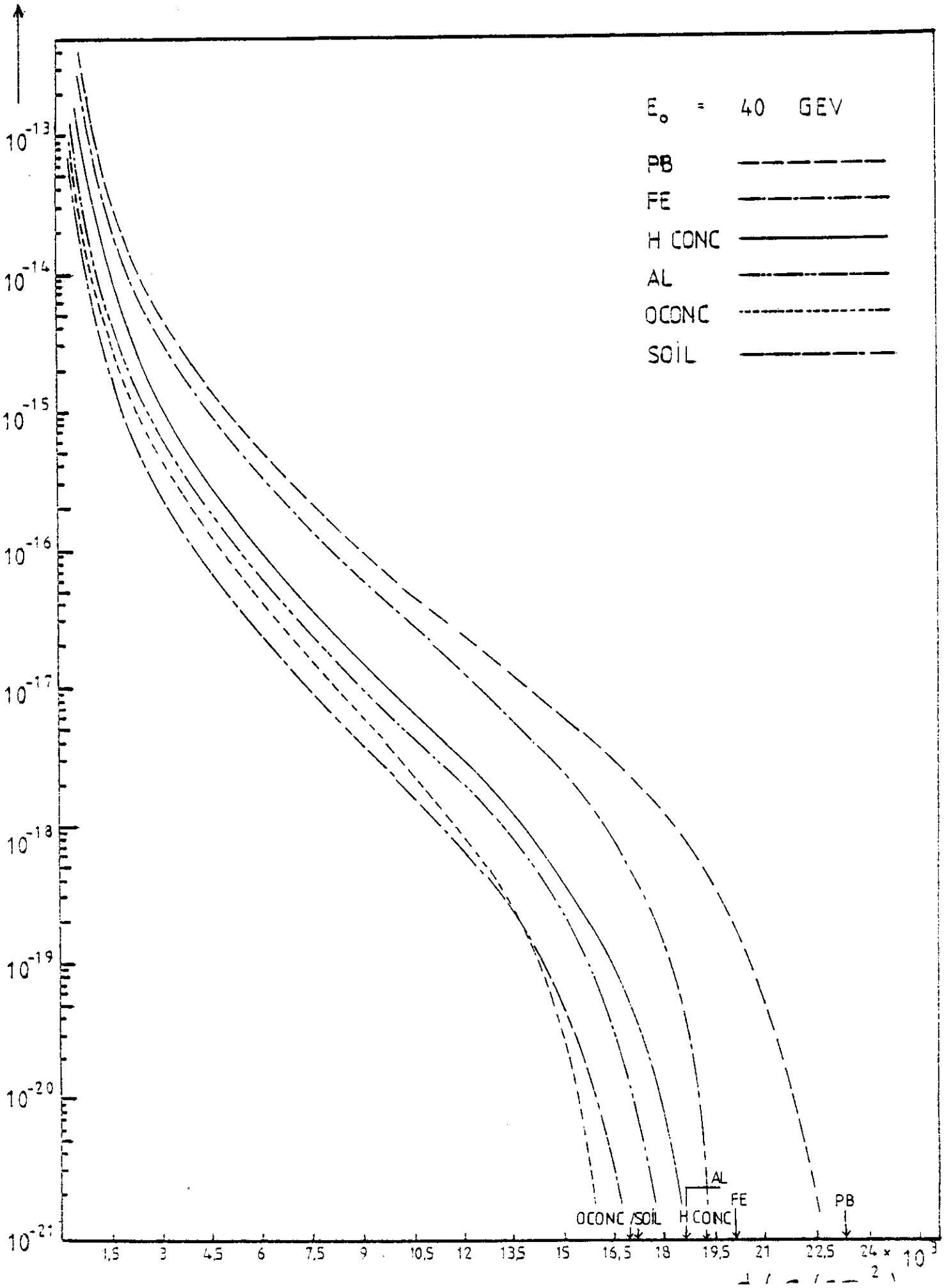
DOSE (cGray/e⁻)
$E_o$ = 40 GEV
PB
FE
H CONC
AL
OCONC
SOIL
$10^{-13}$
$10^{-14}$
$10^{-15}$
$10^{-16}$
$10^{-17}$
$10^{-18}$
$10^{-19}$
$10^{-20}$
$10^{-21}$
1,5
3
4,5
6
7,5
9
10,5
12
13,5
15
16,5
18
19,5
21
22,5
24 × $10^3$
$g/cm^2$
AL
FE
PB
OCONC /SOIL
H CONC

FIG. 12

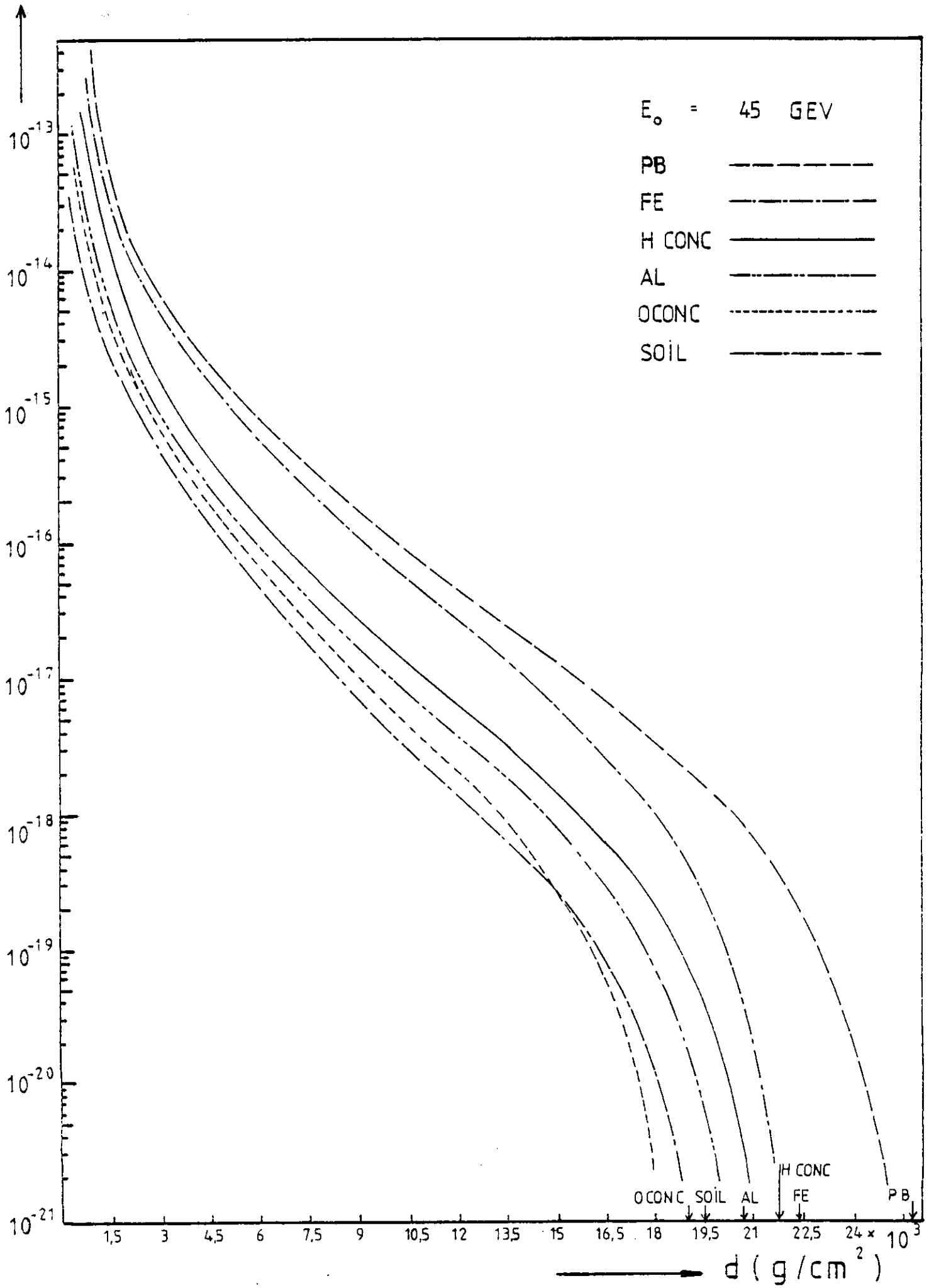
DOSE (cGray/e⁻)
$E_o$ = 45 GEV
PB
FE
H CONC
AL
OCONC
SOIL
$10^{-13}$
$10^{-14}$
$10^{-15}$
$10^{-16}$
$10^{-17}$
$10^{-18}$
$10^{-19}$
$10^{-20}$
$10^{-21}$
1,5
3
4,5
6
7,5
9
10,5
12
13,5
15
16,5
18
19,5
21
22,5
24 × $10^3$
d ( g/cm$^2$ )

FIG. 13

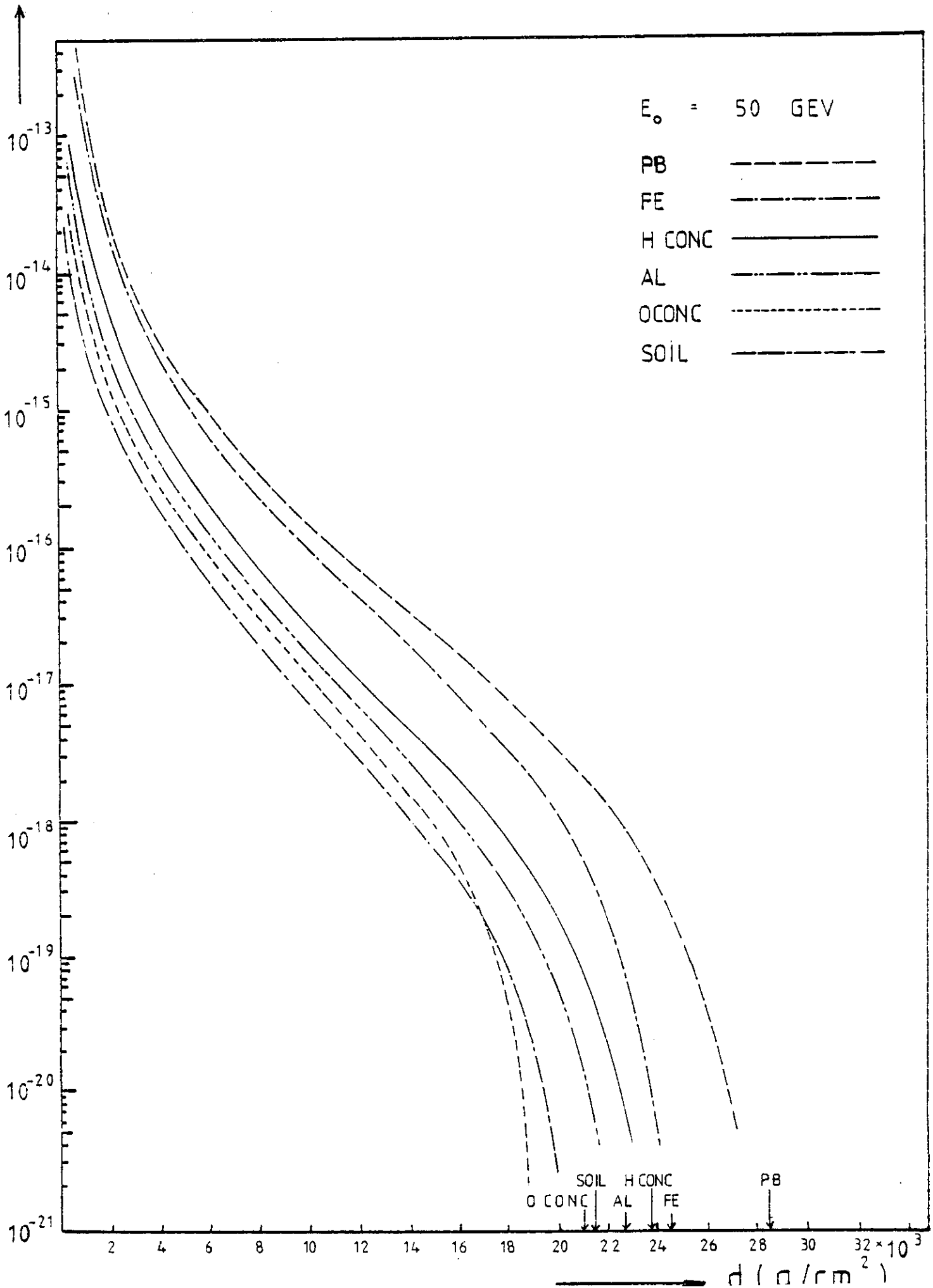
DOSE (cGray/e⁻)
E₀ = 50 GEV
PB
FE
H CONC
AL
OCONC
SOIL
10⁻¹³
10⁻¹⁴
10⁻¹⁵
10⁻¹⁶
10⁻¹⁷
10⁻¹⁸
10⁻¹⁹
10⁻²⁰
10⁻²¹
SOIL
H CONC
PB
O CONC
AL
FE
2 4 6 8 10 12 14 16 18 20 22 24 26 28 30 32 × 10³
d (g/cm²)

FIG. 14

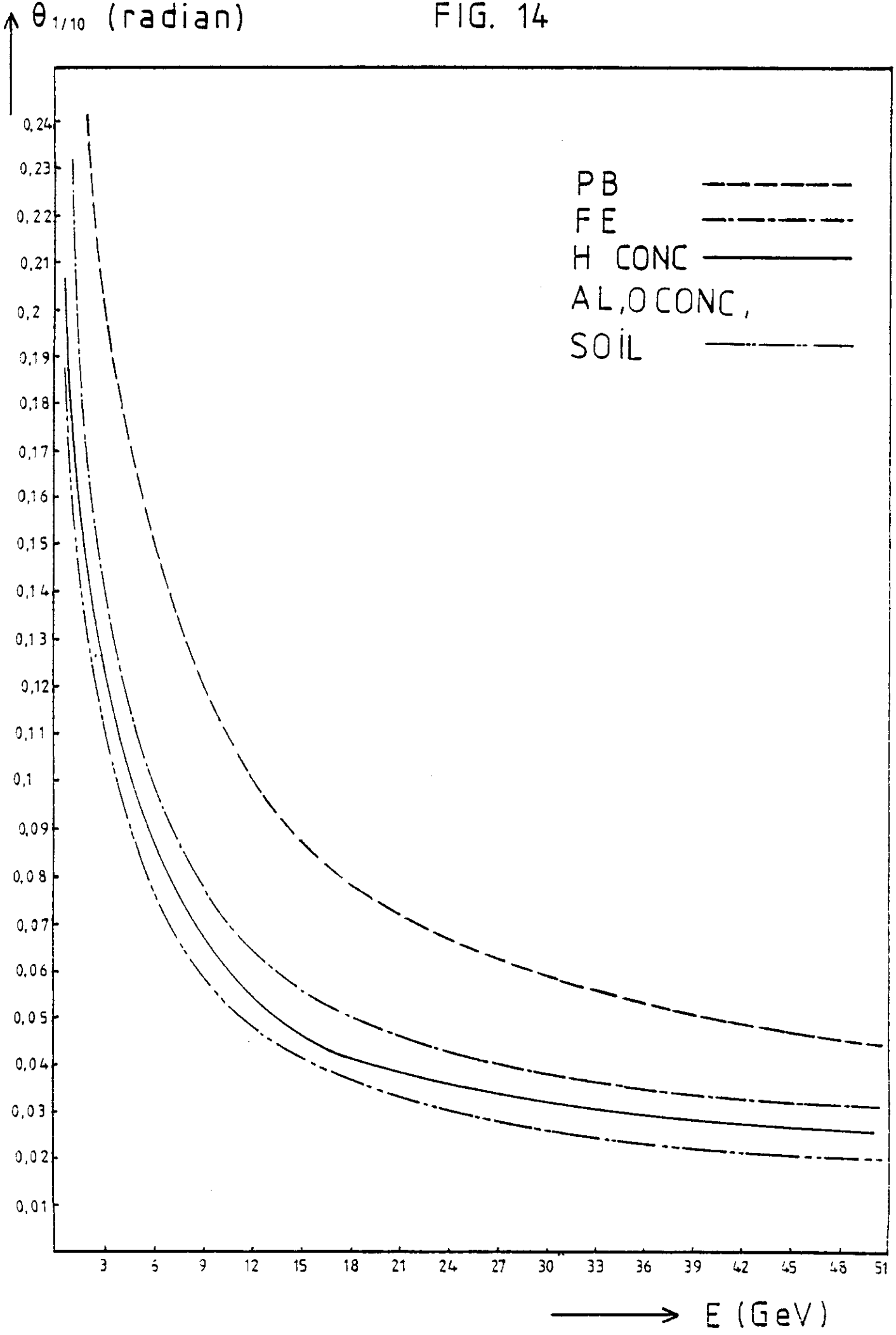
θ 1/10 (radian)
0,24
0,23
0,22
0,21
0,2
0,19
0,18
0,17
0,16
0,15
0,14
0,13
0,12
0,11
0,1
0,09
0,08
0,07
0,06
0,05
0,04
0,03
0,02
0,01
PB
FE
H CONC
AL,O CONC,
SOIL
3
6
9
12
15
18
21
24
27
30
33
36
39
42
45
48
51
E (GeV)

FIG. 15

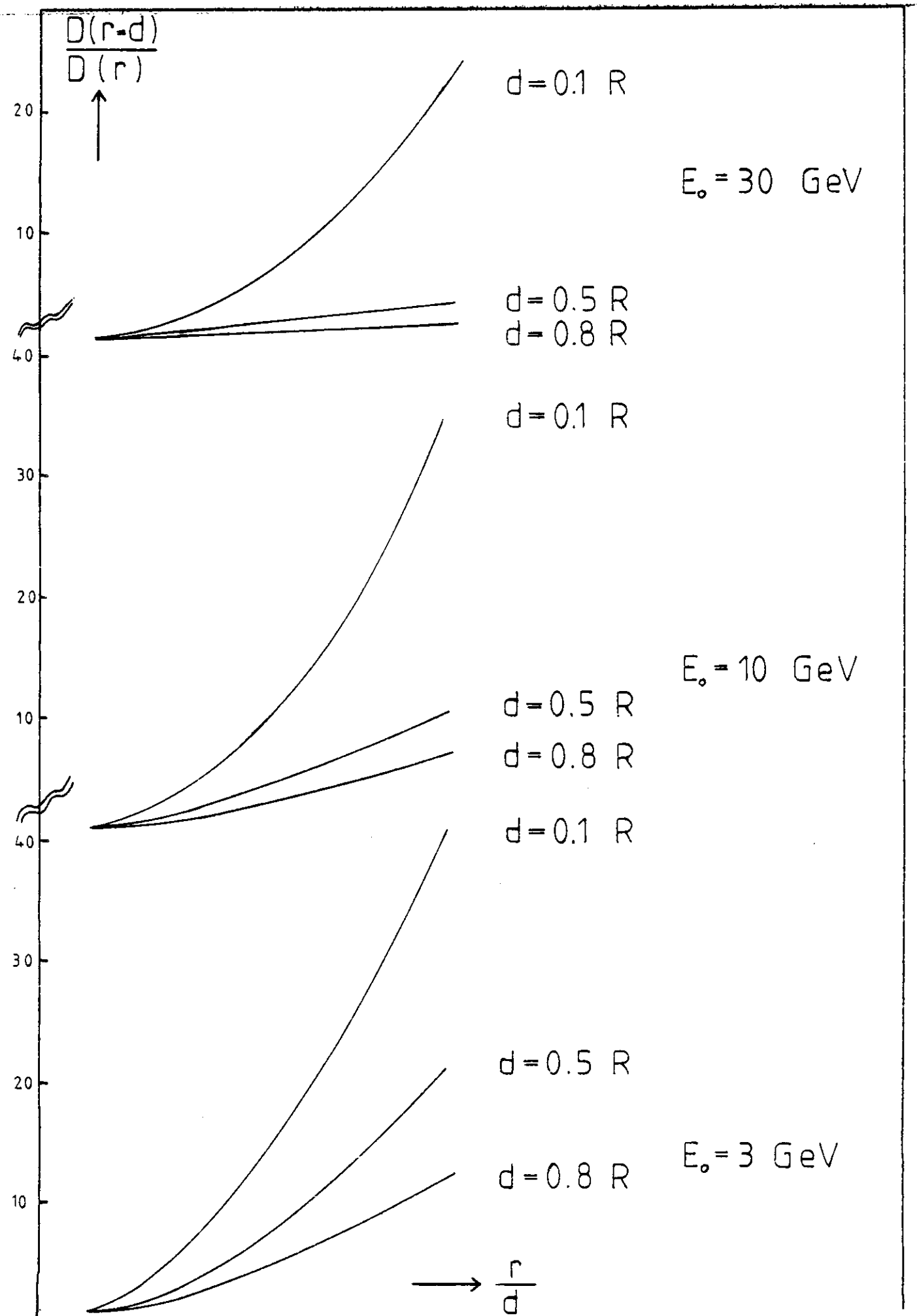
D(r-d)/D(r)
20
10
40
30
20
10
40
30
20
10
d = 0.1 R
E₀ = 30 GeV
d = 0.5 R
d = 0.8 R
d = 0.1 R
E₀ = 10 GeV
d = 0.5 R
d = 0.8 R
d = 0.1 R
E₀ = 3 GeV
d = 0.5 R
d = 0.8 R
r/d

FIG. 16

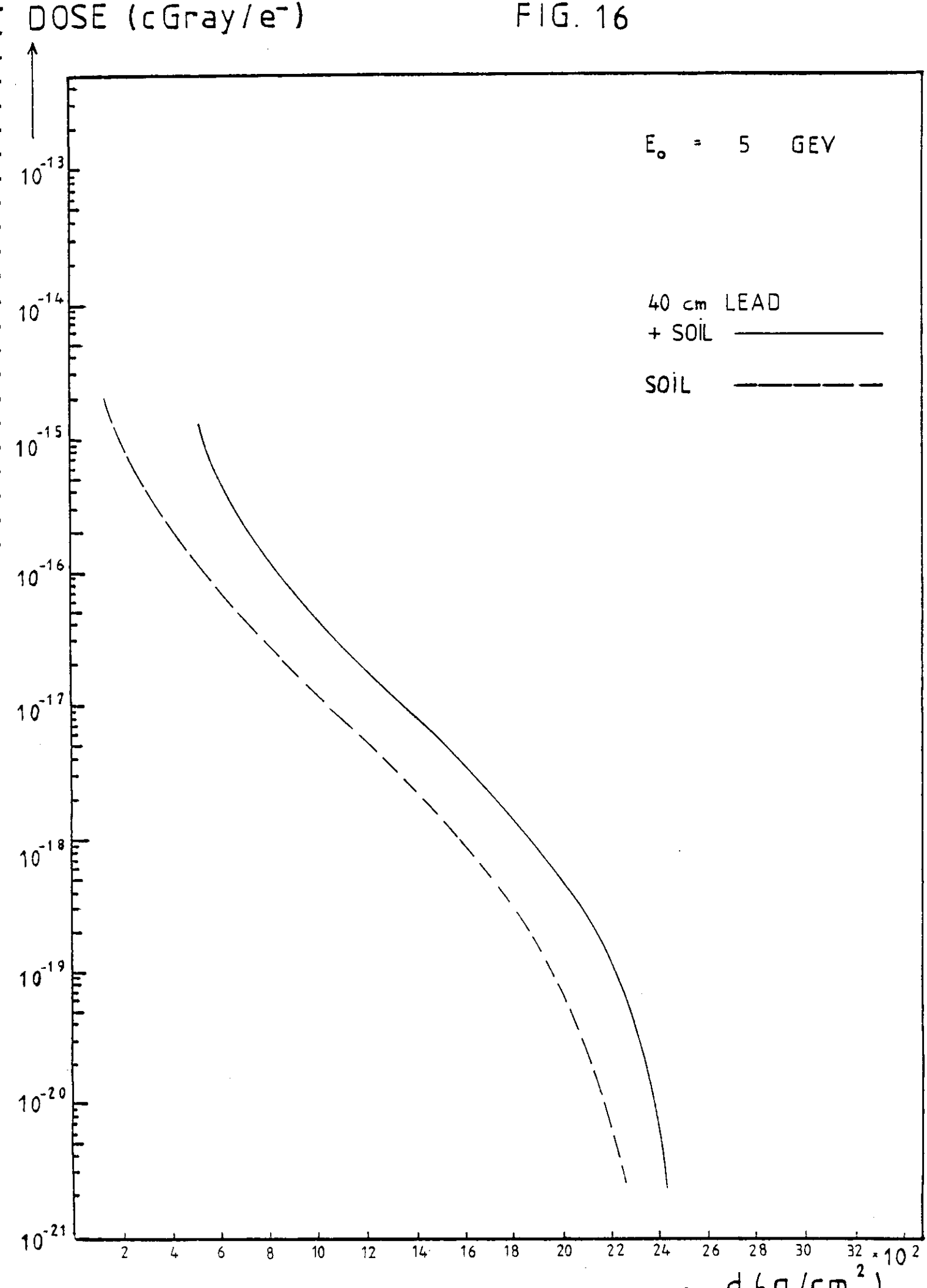
DOSE (cGray/e⁻)
$E_o$ = 5 GEV
40 cm LEAD + SOIL
SOIL
$10^{-13}$
$10^{-14}$
$10^{-15}$
$10^{-16}$
$10^{-17}$
$10^{-18}$
$10^{-19}$
$10^{-20}$
$10^{-21}$
2 4 6 8 10 12 14 16 18 20 22 24 26 28 30 32 $\times 10^2$
$d\,g/cm^2$

FIG. 17

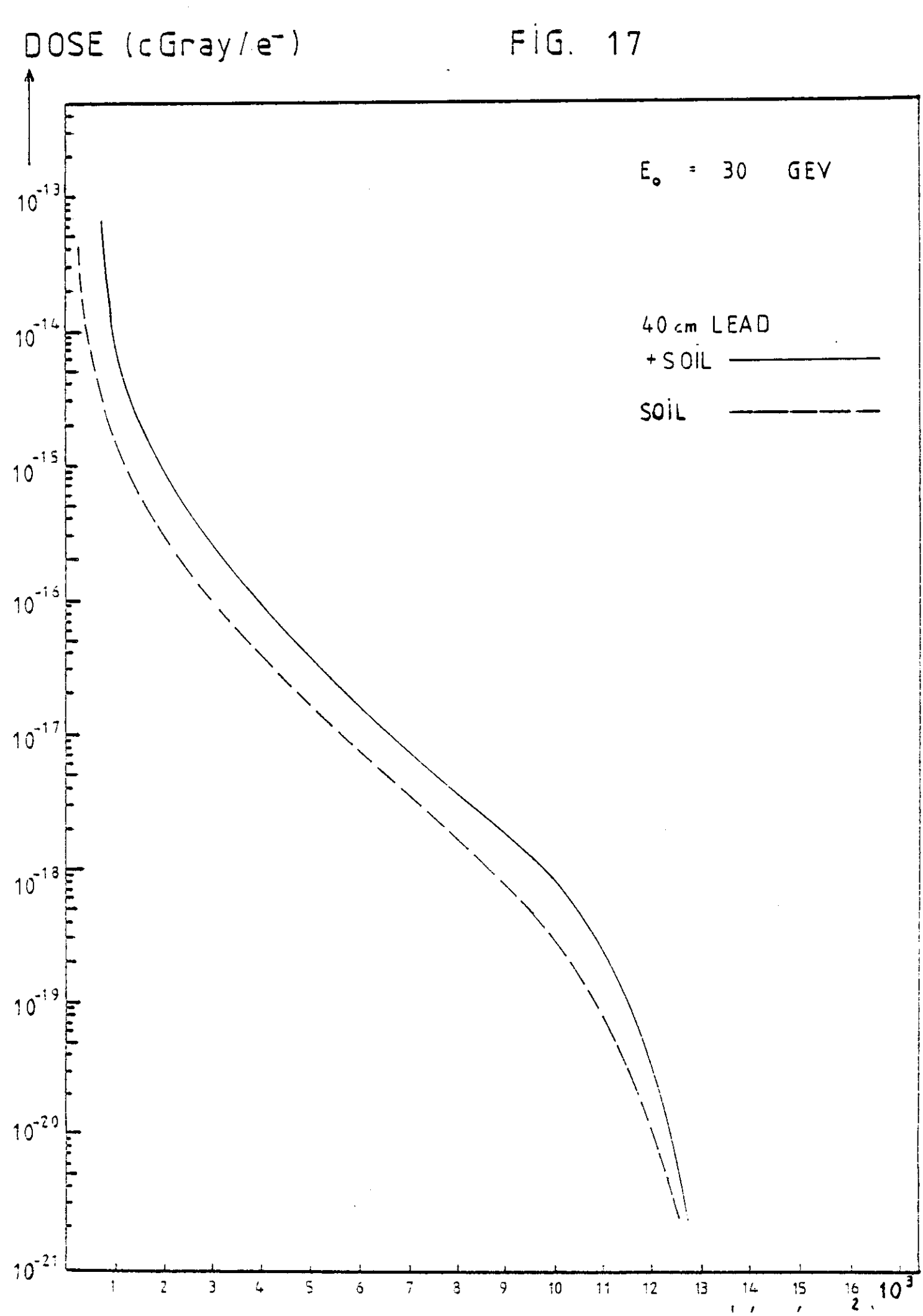
DOSE (cGray/e⁻)
E₀ = 30 GEV
40 cm LEAD
+ SOIL
SOIL
10⁻¹³
10⁻¹⁴
10⁻¹⁵
10⁻¹⁶
10⁻¹⁷
10⁻¹⁸
10⁻¹⁹
10⁻²⁰
10⁻²¹
1
2
3
4
5
6
7
8
9
10
11
12
13
14
15
16
10³

FIG. 18

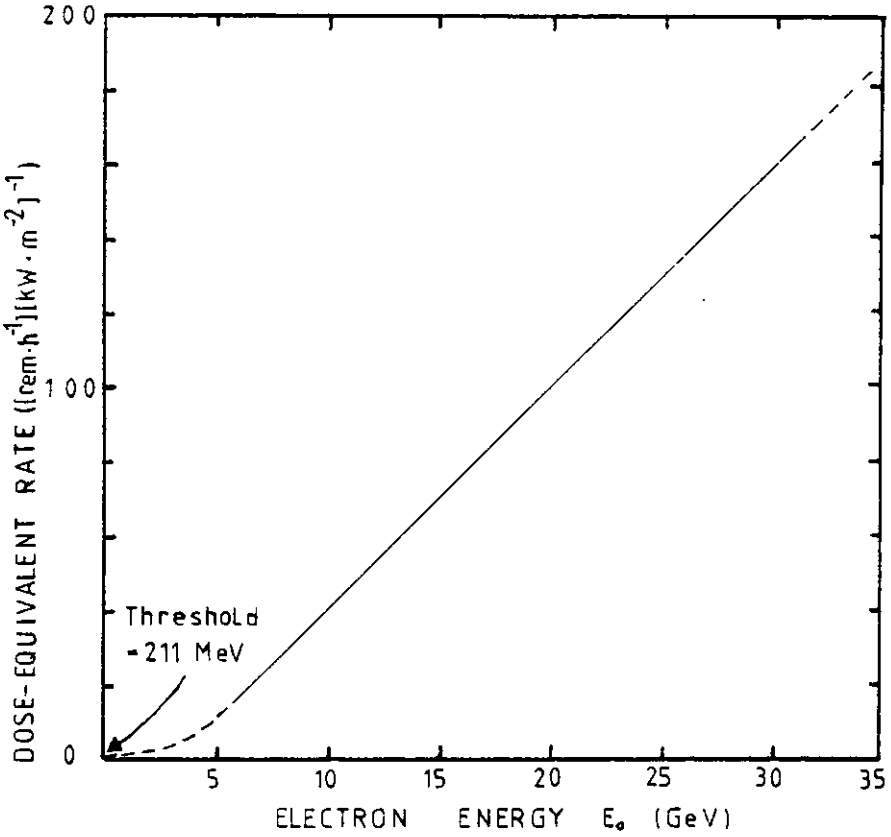
200
100
0
DOSE-EQUIVALENT RATE ([rem·h⁻¹][kW·m⁻²]⁻¹)
Threshold
=211 MeV
5
10
15
20
25
30
35
ELECTRON ENERGY E₀ (GeV)